

## Article

# Sequential Abatement of Fe<sup>II</sup> and Cr<sup>VI</sup> Water Pollution by Use of Walnut Shell-Based Adsorbents

Marius Gheju <sup>1,\*</sup>  and Ionel Balcu <sup>2</sup>

<sup>1</sup> Faculty of Industrial Chemistry and Environmental Engineering, Politehnica University Timisoara, Bd. V. Parvan Nr. 6, 300223 Timisoara, Romania

<sup>2</sup> National Institute for Research and Development in Electrochemistry and Condensed Matter, Str. Dr. Aurel Paunescu Podeanu Nr. 144, 300587 Timisoara, Romania; incemc@incemc.ro

\* Correspondence: marius.gheju@upt.ro; Tel.: +0040-256-404185; Fax: 0040-256-403060

**Abstract:** In this study walnut shells, an inexpensive and readily available waste, were used as carbonaceous precursor for preparation of an innovative adsorbent (walnut-shell powder (WSP)) which was successfully tested for the removal of Fe<sup>II</sup> from synthetic acid mine drainage (AMD). Then, the exhausted iron-contaminated adsorbent (WSP-Fe<sup>II</sup>) was recovered and treated with sodium borohydride for the reduction of adsorbed Fe<sup>II</sup> to Fe<sup>0</sup>. The resulting material (WSP-Fe<sup>0</sup>) was subsequently tested for the removal of Cr<sup>VI</sup> from aqueous solutions. Treatability batch experiments were employed for both Fe<sup>II</sup> and Cr<sup>VI</sup>-contaminated solutions, and the influence of some important experimental parameters was studied. In addition, the experimental data was interpreted by applying three kinetic models and the mechanism of heavy metal removal was discussed. The overall data presented in this study indicated that fresh WSP and WSP-Fe<sup>0</sup> can be considered as promising materials for the removal of Fe<sup>II</sup> and Cr<sup>VI</sup>, respectively. Furthermore, the present work clearly showed that water treatment residuals may be converted in upgraded materials, which can be successfully applied in subsequent water treatment processes. This is an example of sustainable and environmentally-friendly solution that may reduce the adverse effects associated with wastes and delay expensive disposal methods such as landfilling or incineration.



**Citation:** Gheju, M.; Balcu, I. Sequential Abatement of Fe<sup>II</sup> and Cr<sup>VI</sup> Water Pollution by Use of Walnut Shell-Based Adsorbents. *Processes* **2021**, *9*, 218. <https://doi.org/10.3390/pr9020218>

Received: 20 December 2020

Accepted: 22 January 2021

Published: 25 January 2021

**Publisher's Note:** MDPI stays neutral with regard to jurisdictional claims in published maps and institutional affiliations.



**Copyright:** © 2021 by the authors. Licensee MDPI, Basel, Switzerland. This article is an open access article distributed under the terms and conditions of the Creative Commons Attribution (CC BY) license (<https://creativecommons.org/licenses/by/4.0/>).

**Keywords:** sustainable water treatment; water treatment residuals; innovative adsorbent; heavy metals; acid mine drainage; hexavalent chromium

## 1. Introduction

In last decades, water pollution with heavy metals has become an increasingly important worldwide threat. Numerous heavy metals have been introduced into natural water environments, especially as a result of human industrial activities, but also due to agricultural, transport and waste disposal practices. Among the most important industrial activities that contribute to contamination of aquatic systems by metallic ions (Cr, Ni, Zn, Cu, Zn, Pb, Fe, Cd etc.) are: electroplating, surface finishing of metals, production and recycling of electronics, metallurgy, mining, leather tanning, paper and pulp production, fertilizer and pesticide production, batteries production [1–4]. Most heavy metals cause toxic effects to living species, not only at excessive exposures, but also at low concentrations, because they do not have any biological role in living cells, do not degrade into harmless end products, and are bioaccumulative in nature. In addition, even heavy metals which are necessary in small amounts as micronutrients for the normal development of biological systems (e.g., Cu, Fe, Zn, Cr etc.) exert harmful effects to biological organisms at high concentrations [4–6]. Therefore, the removal of heavy metals from contaminated waters, prior to their discharge into natural effluents, is a necessary step in order to reduce their adverse effects. The World Health Organization guidelines of some heavy metals in drinking water are summarized in Table S1.

Various methods have been applied for the removal of heavy metals from aqueous solutions; these include chemical precipitation, membrane technologies, ion exchange, electrochemical treatment, floatation, coagulation-flocculation, adsorption, evaporation, photocatalysis [1,3,7–11]. Among all these methods, adsorption is generally considered to be one of the best for the removal of heavy metals, due to its simplicity, ease of operation, selectivity and high efficiency. Activated carbon is the most widely used adsorbent in water and wastewater treatment, owing to its high surface area and high degree of surface porosity and reactivity. The heavy metal adsorption capacities reported in the literature for commercial activated carbon are in the range of 0.29–146 mg/g [12]. Unfortunately, in spite of its excellent adsorption capacity, this material is also expensive, which makes the costs of adsorption processes high, and, therefore, less economically viable, especially in low income developing countries [4,13,14]. Therefore, over the last decades, there has been an intense activity directed at the development of inexpensive and easily available alternatives to commercially available activated carbon (e.g., clay minerals, industrial/agricultural wastes/byproducts etc.) which should decrease the cost of the adsorption process, while still being efficient in improving the quality of the treated effluents [3,4,14–19]. The heavy metal adsorption capacities reported in [12] for natural materials, agricultural and industrial wastes are in the range of 0.003–83.3, 0.001–158 and 0.0002–133.35 mg/g, respectively; thus, it is obvious that low-cost adsorbents may exert excellent metal removal capabilities, comparable to commercial activated carbon [12].

On the other hand, water treatment technologies should be not only efficient and affordable, but also environmental-friendly. Therefore, great attention has been paid in the last years to handling and disposal of water treatment residues (WTRs), which are challenging tasks for today environmental scientists. One of the traditional and most common methods of WTR management is by landfilling. However, today, this is no longer considered a viable solution because of: (1) soil and groundwater contamination, (2) high operating costs, and (3) difficulties in finding and operating new landfill sites, under the circumstances of more and more strict environmental regulation. Hence, recovery, recycling and reuse should be the preferred solution for the sustainable management of WTR [20]. The use of groundwater treatment residuals (Fe and Mn (hydr)oxides) and flocculation-coagulation residuals (Fe and Al (hydr)oxides) as adsorbents, to remove pollutants (e.g., heavy metals, metalloids, pesticides etc.) from aqueous solutions, has been reported in the last years by numerous studies [21–24]. Instead, to our knowledge, few researchers have addressed the issue of reusability of cheap exhausted adsorbents, resulted from the removal of a particular heavy metal, in treatment processes of aqueous effluents polluted with a different type of heavy metal [25]. In this previous study, bentonite was used for sequential adsorption of heavy metals from aqueous solutions, proving not only that reusability of exhausted adsorbents is possible, but also that some adsorbed metals may have a beneficial role in the subsequent adsorption process. However, this research also revealed that using bentonite as adsorbent suffers from multiple drawbacks, including low adsorption capacity and leaching of structural iron at strong acidic pH [25].

The fruit and vegetable processing industry operates globally, producing huge amounts of products and being a well-known generator of large volumes of agricultural wastes [26,27]. The world production of walnuts has been relatively stable over the last years, at about 2 million tons (in-shell basis), with China and the USA accounting for nearly three-quarters of the total production [28]. Since the kernel represents approximately 45% of the walnut mass (depending on the size and the variety of the walnut), it is obvious that the remaining shells are an abundantly available waste that could be used as cheap adsorbent materials. Consequently, the present study has two main objectives. Firstly, to investigate the use of walnut shells, in powdered form (WSP), as cheap adsorbent in the remediation process of synthetic acid mine drainage (AMD) containing  $\text{Fe}^{\text{II}}$ . To the best of our knowledge, removal of  $\text{Fe}^{\text{II}}$  with agricultural waste derived adsorbents are few [29,30], while walnut shells in their natural form (i.e., not activated by any chemical or physical method) were not researched yet. The second objective of this paper was to recover the water treatment residue

(WSP-Fe<sup>II</sup>) resulted from the AMD remediation process, for further reuse in the removal of Cr<sup>VI</sup> from aqueous solutions. Since during the last two decades Fe<sup>0</sup> was acknowledged as an efficient reactive material for remediation of heavy metal contaminated effluents [31], the water treatment residue (WSP-Fe<sup>II</sup>) resulted from AMD remediation was treated with sodium borohydride, in order to reduce the adsorbed Fe<sup>II</sup> to Fe<sup>0</sup>, and the resulted material (WSP-Fe<sup>0</sup>) was then used for the removal of Cr<sup>VI</sup>. The effect of several important experimental parameters (pH, heavy metal concentration, temperature, and ionic strength) on efficiency of both treatment processes was investigated. Furthermore, the kinetic parameters of the remediation processes were determined and the mechanisms of Fe<sup>II</sup> and Cr<sup>VI</sup> removal were discussed.

## 2. Results and Discussion

### 2.1. Adsorbent Characterization

#### 2.1.1. Fourier-Transform Infrared Spectroscopy (FTIR) Analysis

The FTIR spectra of the adsorbents were recorded within the range of 500–4000 cm<sup>-1</sup>. The spectra of native WSP and WSP-Fe<sup>II</sup> are given in Figures S1 and S2 (Supplementary Material). The analysis of Figure S1 reveals a wide band near 3440 cm<sup>-1</sup>, indicating the presence of hydrogen-bonded hydroxyl groups on the WSP surface [32]. This can be correlated with the intense band around 1040 cm<sup>-1</sup>, characteristic for the valence vibration of C-O bond in primary alcohols [33,34]. Peaks observed around 2920 and 1380 cm<sup>-1</sup> can be assigned to the stretching vibration of C-H bonds in methyl and methylene groups [35]. The flat peak located at about 2100–2200 cm<sup>-1</sup> corresponds to C≡C groups stretching vibration [34]. The bands around 1750 and 1720 cm<sup>-1</sup> are indicative for the C=O group stretching vibration in carboxyl and carbonyl groups [35,36]. Peaks around 1370 and 1330 cm<sup>-1</sup> may be attributed to the O-H in-plane deformation characteristic for alcohols and phenols [33,37]. Absorption bands near 1650, 1600, 1510, 1260, 800, 670 and 600 cm<sup>-1</sup> can be related to complex vibrations related to aromatic compounds (e.g., lignin) [32–35,37]. By comparing the spectra of WSP (Figure S1) and WSP-Fe<sup>II</sup> (Figure S2), a strong decrease in intensity of peaks at 3440, 1600, 1260, 1040 and 800 cm<sup>-1</sup> could be observed after the adsorption of Fe<sup>II</sup>; if we assume that FTIR spectra were recorded by following the same procedure (i.e., pellets were prepared by mixing and pressing exactly the same amounts of sample and KBr), this may suggest participation of some of the above mentioned functional groups (hydroxyl, carboxyl and carbonyl) in metal binding. Similar changes in intensity of the bands was observed also after the reaction of Cr<sup>VI</sup> solution with WSP and WSP-Fe<sup>0</sup> (Figures S1, S3–S5, Supplementary Material).

#### 2.1.2. Scanning Electron Microscopy (SEM) Analysis

The SEM analysis enables the observation of the surface morphology of the studied adsorbents materials. Visual examination of the SEM micrographs (Figures S6–S10, Supplementary Material) showed that external surface of prepared materials has an irregular rugged morphology, containing macropores with sizes of 1–2 μm, homogeneously distributed all over the surface. No noticeable differences can be observed in SEM micrographs before and after the adsorption process; no accumulation of contaminant on the exhausted adsorbent can be discerned too, presumably due to the low amount of retained metal at surface of the adsorbents.

#### 2.1.3. Energy Dispersive X-ray Spectroscopy Analysis (EDX) Analysis

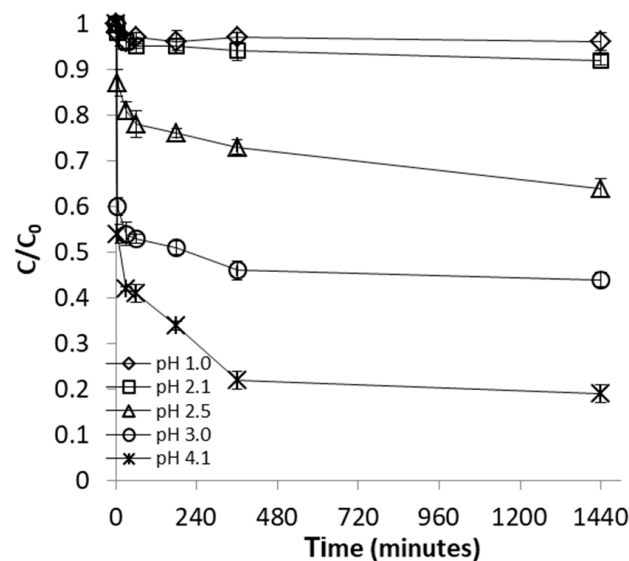
The EDX spectra of the adsorbents before and after Cr<sup>VI</sup> adsorption are shown in Figures S11–S15 (Supplementary Material). The absence of alkali and alkaline earth metals (Ca<sup>2+</sup> and K<sup>+</sup>) in the WSP-Fe<sup>II</sup> sample (Figure S10) indicated that the adsorption process may have involved an ion-exchange mechanism; furthermore, the EDX spectra of WSP-Fe<sup>II</sup> revealed additional Fe signals in comparison to WSP, indicating retention of Fe at the surface of adsorbent. The EDX analysis also confirmed the retaining of Cr<sup>VI</sup> onto the surface of both WSP (control experiments) and WSP-Fe<sup>0</sup>; nevertheless, a visual comparison

of EDX spectra of Cr<sup>VI</sup>-loaded WSP-Fe<sup>0</sup> and WSP (Figures S14 and S15) clearly reveals that more Cr was bound on WSP-Fe<sup>0</sup>. In addition, the suppression of one Fe band in the EDX spectra of WSP-Fe<sup>0</sup> after reaction with Cr<sup>VI</sup> may suggest that the Fe<sup>0</sup> sites were involved in removal of Cr<sup>VI</sup> anions.

## 2.2. AMD Treatability Experiments

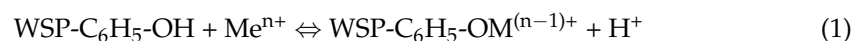
### 2.2.1. Effect of pH

Earlier studies have shown that pH of the aqueous solution is a highly important factor in adsorption processes, capable to control the mechanism, and therefore, to enhance or decrease the amount of metal retained at the adsorbent surface [38]. The effect of pH on the removal of Fe<sup>II</sup> was studied by varying the pH of the metal ion solution from 1.0 to 4.1. These pH values were selected because they are within the range of levels reported for pH in AMD environments [39,40]. In addition, pH values below 4.5 also ensure that removal of Fe<sup>II</sup> occurs solely due to adsorption. Figures 1 and 2 clearly show that both efficiency of Fe<sup>II</sup> removal and adsorption capacity of WSP increased with increasing pH from 1.0 to 4.1. While only limited AMD remediation was observed at pH 1.0 and 2.1, an important enhancement of the adsorption process was achieved as pH was increased to 2.5, and then further gradually raised up to 4.1. This is in accord with results of previous works using alternative vegetal adsorbents like thermochemically-activated walnut shells and orange peels, which indicated increased removal efficiency with increasing pH of the solution [29,30].



**Figure 1.** Effect of pH on Fe<sup>II</sup> removal by walnut-shell powder WSP. The lines are not fitting models; they simply connect points to facilitate visualization.

Carboxyl and hydroxyl (fenolic) groups are among the most important functional oxidized groups (active centers) existent at surface of natural carbon-based agricultural residues, which are able to take part in specific adsorption processes with metal cations, according to [20,41]:



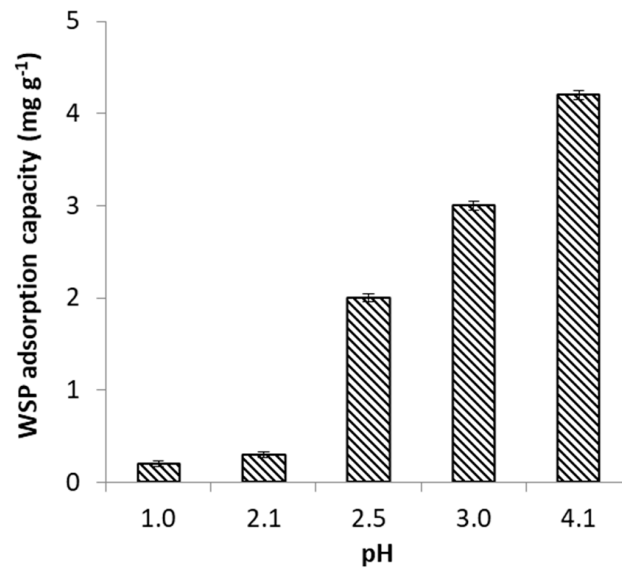
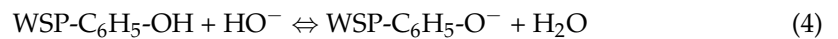
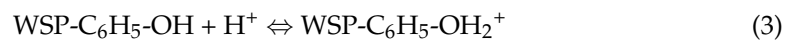


Figure 2. Effect of pH on Fe<sup>II</sup> adsorption capacity of WSP.

However, carboxyl and hydroxyl groups are also involved in acido-basic equilibria which may be described as following:



In the present work, the  $\text{pH}_{\text{pzc}}$  of the WSP was found to be 6.4; accordingly, the net charge of WSP surface was positive over the entire studied pH range. Nevertheless, it is clear from the above equations that an increase in solution pH (i.e., more  $\text{HO}^-$  anions available for Equations (4) and (6)) causes an increase in the number of negative charges existent at WSP surface, even though the net charge still remains positive at  $\text{pH} < 6.4$ . Hence, on the one hand, the efficiency of adsorption will increase at higher pH due to enhanced electrostatic attraction between cationic Fe<sup>II</sup> species and negatively charged centers at WSP surface. On the other hand, the competition with hydronium cations for anionic exchanging sites at WSP surface also decreased as the pH was raised in the range 1.0–4.1, contributing thus to the increased sorption of Fe<sup>II</sup> cations.

### 2.2.2. Effect of Fe<sup>II</sup> Initial Concentration

The influence of Fe<sup>II</sup> concentration was studied within the concentration range of 25–100 mg L<sup>-1</sup>. These concentrations were selected because they are within the range of Fe<sup>II</sup> levels reported in AMD environments [39,40]. As revealed in Figure 3, the efficiency of Fe<sup>II</sup> uptake by WSP was found to decrease proportionally with the increase of Fe<sup>II</sup> concentration. This is attributable to the fact that available sorption sites become progressively insufficient for the increasingly number of Fe<sup>II</sup> ions at higher concentrations; hence, a more rapid saturation of the adsorption centers will occur and, as a result, the percentage removal of Fe<sup>II</sup> ions decreases. Figure 3 also shows that adsorption of Fe<sup>II</sup> proceeds in two steps: a rapid decrease of metal concentration within the first stage (first 60 min), when the amount of available sites was still much higher than the amount of Fe<sup>II</sup> ions to be adsorbed, followed by a strong decrease in the adsorption rates in the second phase, due to continuous diminishing of the number of negatively charged functional groups throughout the adsorption experiment. This phenomenon was previously reported by several studies employing agro-based waste adsorbents in the process of heavy metal removal from aque-

ous solutions [16]. In contrast, Figure 4 indicates that adsorption capacity of WSP firstly increased with increasing the initial  $\text{Fe}^{\text{II}}$  concentration, and then reached a saturation value. The maximal adsorption capacity of WSP was found to be about  $5.8 \text{ mg g}^{-1}$ , achieved at the concentration of  $100 \text{ mg L}^{-1} \text{ Fe}^{\text{II}}$ . The higher amount of  $\text{Fe}^{\text{II}}$  retained per unit mass of adsorbent ( $\text{mg g}^{-1}$ ) at higher initial concentration is the result of increased  $\text{Fe}^{\text{II}}$  concentration gradient at solution-adsorbent interface (i.e., increased probability of collision between metal ions and adsorbent surface), which led to enhanced mass transfer driving forces to overcome all mass transfer resistances [42]. Our results are in agreement with findings reported by several earlier workers for  $\text{Fe}^{\text{II}}$  adsorption on agro-wastes, such as thermochemically-activated walnut shells and orange peels [29,30].

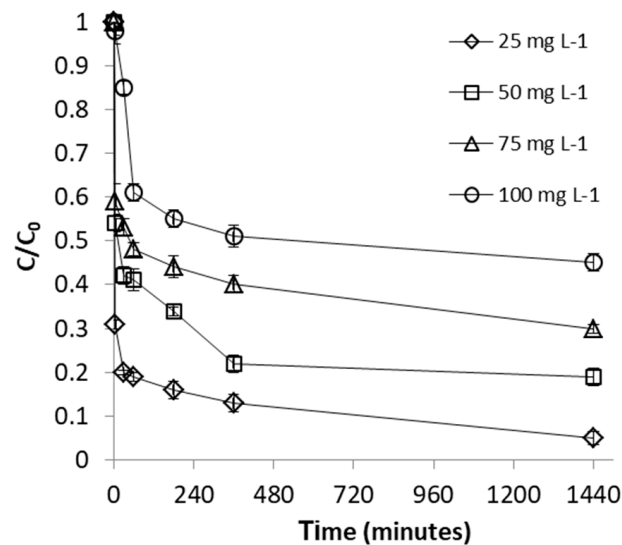


**Figure 3.** Effect of initial concentration on  $\text{Fe}^{\text{II}}$  removal by WSP. The lines are not fitting models; they simply connect points to facilitate visualization.

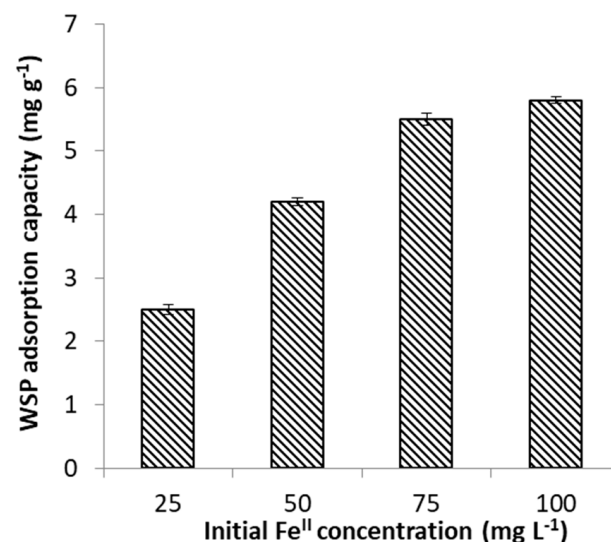


**Figure 4.** Effect of initial concentration on  $\text{Fe}^{\text{II}}$  adsorption capacity of WSP.

### 2.2.3. Effect of Temperature

The effect of temperature was investigated over the range of 6–33 °C. The results presented in Figures 5 and 6 show that uptake of  $\text{Fe}^{\text{II}}$  on WSP was positively affected by the increase of temperature; nevertheless, it is important to point out that an improvement in  $\text{Fe}^{\text{II}}$  adsorption was observed only when temperature was increased from 6 to 22 °C;

a subsequent rise of temperature to 33 °C led to no discernible enhancement the Fe<sup>II</sup> uptake. The observed temperature dependence is indicative of an endothermic adsorption process. The enhancement of adsorption efficacy with increasing temperature may be attributed to better interactions between Fe<sup>II</sup> and WSP as a result increased rates of intraparticle diffusion of Fe<sup>II</sup> ions into the pores of WSP, or to creation of new adsorption sites at higher temperatures [43]. The positive effect of temperature on the adsorption efficacy was reported also in early works investigating removal of Fe<sup>II</sup> from aqueous solutions by adsorption on thermochemically-activated walnut shells and orange peels [29,30].

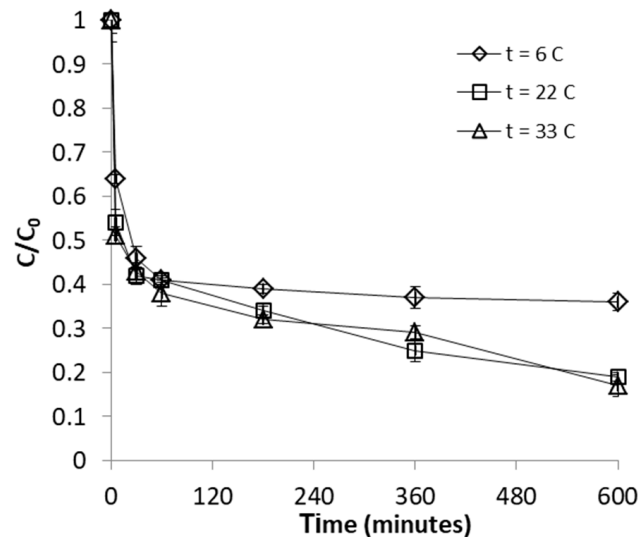


**Figure 5.** Effect of temperature on Fe<sup>II</sup> removal by WSP. The lines are not fitting models; they simply connect points to facilitate visualization.

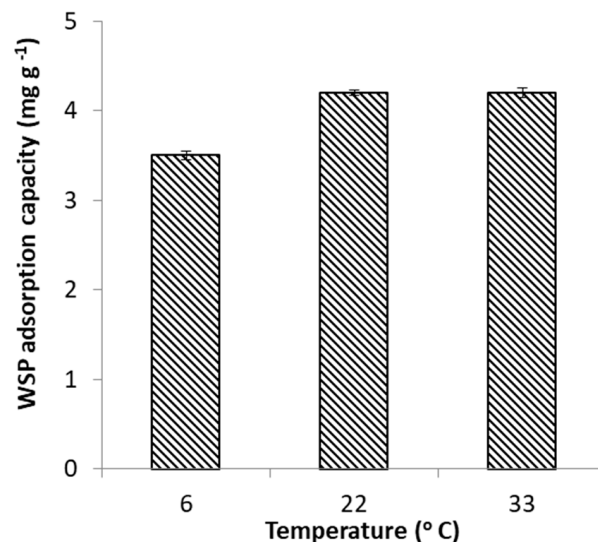


**Figure 6.** Effect of temperature on Fe<sup>II</sup> adsorption capacity of WSP.

#### 2.2.4. Effect of Ionic Strength

To investigate the influence of ionic strength, adsorption of Fe<sup>II</sup> on WSP was conducted in the co-presence of NaCl concentrations of 0, 0.01, 0.03 and 0.05 M as background electrolyte. NaCl was used as indifferent electrolyte, in accord to previous studies investigating the effect of ionic strength [44]. From Figures 7 and 8 it results that the process of Fe<sup>II</sup> adsorption was progressively hindered in the presence of increasingly concentrations of competing Na<sup>+</sup> cations. The trend of the change of metal adsorption with ionic strength can be used for differentiating between the two main adsorption processes that may be

involved in binding of anions onto minerals: physical (non-specific) adsorption, and chemical (specific) adsorption. In our case, the observed effect can be interpreted as indicating non-specific weak interactions (physisorption) being involved in adsorption mechanism of  $\text{Fe}^{\text{II}}$  [44].

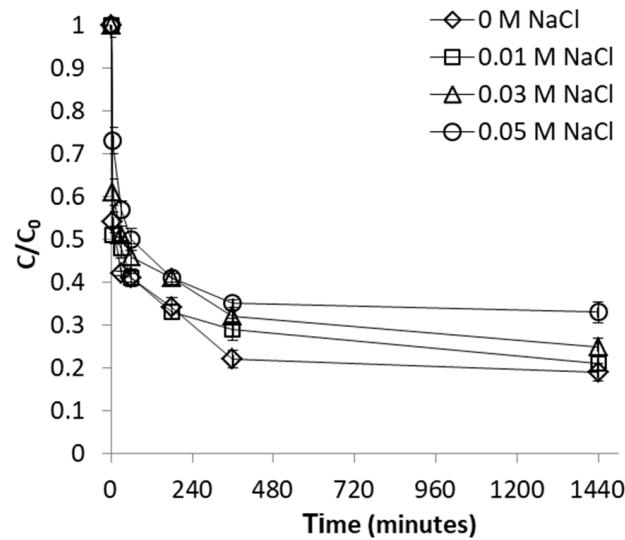


**Figure 7.** Effect of ionic strength on  $\text{Fe}^{\text{II}}$  removal by WSP. The lines are not fitting models; they simply connect points to facilitate visualization.

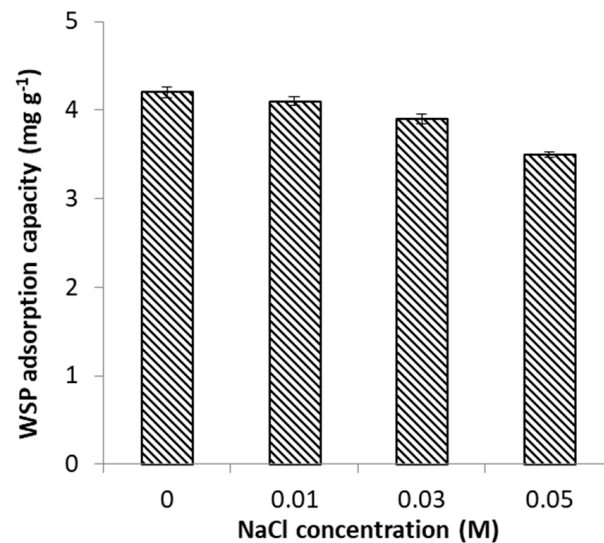


**Figure 8.** Effect of ionic strength on  $\text{Fe}^{\text{II}}$  adsorption capacity of WSP.

### 2.3. $\text{Cr}^{\text{VI}}$ Treatability Experiments

#### 2.3.1. Effect of pH

In this series of tests the impact of initial pH was studied within the pH range of 1.0–5.9. The results of the present experiments (Figure 9) indicated that  $\text{Cr}^{\text{VI}}$  removal with WSP- $\text{Fe}^0$  was significantly hindered by the increase of pH; moreover, at  $\text{pH} \geq 5.1$   $\text{Cr}^{\text{VI}}$  removal was almost totally inhibited. Control experiments with WSP showed the same trend of decreasing efficacy of  $\text{Cr}^{\text{VI}}$  removal with increasing pH (Figure 9). Our results may be attributed, on the one hand, to a decrease in the number of positive charges existent at WSP surface with increasing pH, which hinders electrostatic attraction of anionic  $\text{Cr}^{\text{VI}}$  species. On the other hand, removal of  $\text{Cr}^{\text{VI}}$  at  $\text{Fe}^0$  centers is known to be a complex process also inhibited by the increase of pH [45]. Similar maximum adsorption efficiency in the acidic range has been most often reported in the literature for retaining of  $\text{Cr}^{\text{VI}}$

on adsorbents developed from different agricultural wastes (acid-activated rice husk,  $\text{ZnCl}_2$ -activated wood, acid-activated saw dust,  $\text{ZnCl}_2$ -microwave-activated sawdust, date pits, tea-waste) [32,46–48]. However, different influence of pH has also been observed; for instance, the effective pH range for *Chrysophyllum albidum* seed shells-based adsorbents was found to be 4.5–5 [49].

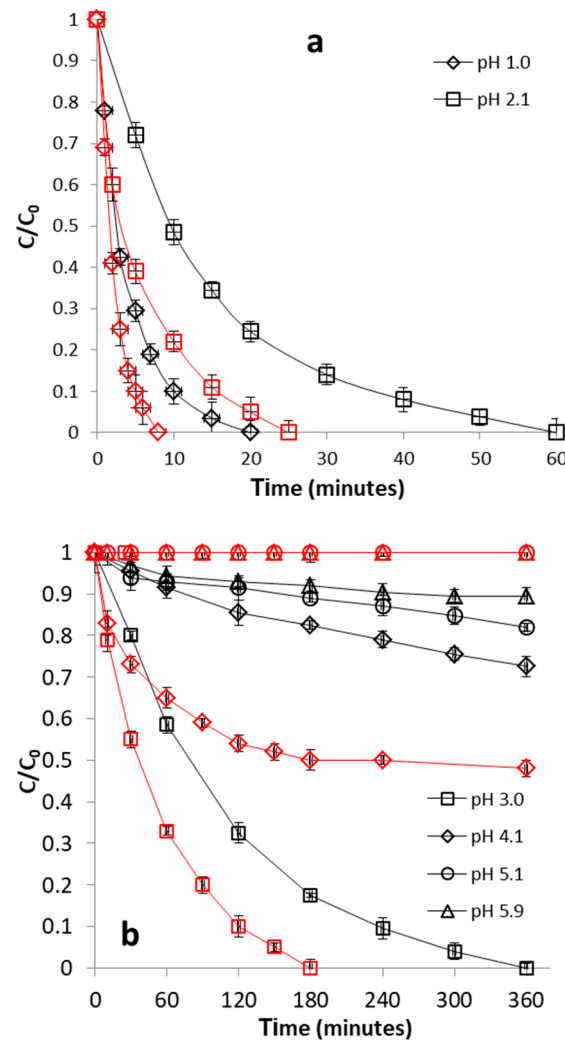


**Figure 9.** Effect of pH on  $\text{Cr}^{\text{VI}}$  removal by WSP- $\text{Fe}^0$  (red curves) and WSP (black curves). (a) pH 1.0–2.1; (b) pH 3.0–5.9. The lines are not fitting models; they simply connect points to facilitate visualization.

Two important observations can be made by analyzing the findings of pH influence experiments: (1) higher  $\text{Cr}^{\text{VI}}$  removal efficiencies for WSP- $\text{Fe}^0$  than for WSP were observed over the pH range of 1.0–4.1, and (2) no  $\text{Cr}^{\text{VI}}$  removal and low  $\text{Cr}^{\text{VI}}$  removal efficiency was noticed over the pH range of 5.1–5.9 for WSP- $\text{Fe}^0$  and WSP, respectively. The existence of  $\text{Fe}^0$  centers at surface of WSP- $\text{Fe}^0$  may explain both the better  $\text{Cr}^{\text{VI}}$  removal at pH 1.0–4.1 and the lack of  $\text{Cr}^{\text{VI}}$  removal at pH 5.1–5.9, observed for WSP- $\text{Fe}^0$ . It is well known that  $\text{Cr}^{\text{VI}}$  removal at  $\text{Fe}^0$  surface (adsorption + possible reduction) is pH-dependent: the lower the pH, the higher the removal efficiency [45]. However,  $\text{Cr}^{\text{VI}}$  adsorption at WSP surface is also favored by an acidic pH. Therefore, it is apparent that adsorption at surface of  $\text{Fe}^0$  centers was more severely hindered at pH 5.1–5.9 than adsorption at surface of WSP surface. This is a relevant evidence of the importance of  $\text{Fe}^0$  centers in the process of  $\text{Cr}^{\text{VI}}$  removal with WSP- $\text{Fe}^0$ .

### 2.3.2. Effect of Cr<sup>VI</sup> Initial Concentration

The influence of initial concentration was examined by varying the initial metal concentration from 1 to 5 mg L<sup>-1</sup>. These concentrations were selected because they are within the common levels both for subsurface Cr<sup>VI</sup>-contaminated groundwater [50] and for wastewater effluents [51,52]. Figure 10 depicts the influence of initial Cr<sup>VI</sup> concentration on removal efficiency. It can be easily seen from this figure that initial concentration of Cr<sup>VI</sup> is another parameter which plays an important role in the process of Cr<sup>VI</sup> removal with WSP-Fe<sup>0</sup>: the higher the initial Cr<sup>VI</sup> concentration, the lower the efficacy of the removal process. The same outcome was noticed also for the control experiments conducted with WSP (Figure 10): uptake of Cr<sup>VI</sup> was inhibited at higher Cr<sup>VI</sup> concentrations; nevertheless, Figure 10 clearly reveals that, for same Cr<sup>VI</sup> initial concentration, better removal yields were always obtained for WSP-Fe<sup>0</sup> than for WSP, which is attributable to existence of Fe<sup>0</sup> at surface of WSP-Fe<sup>0</sup>. The results of the influence of initial concentration are consistent with previous findings reporting removal of Cr<sup>VI</sup> from aqueous effluents by use of other biosorbents (acid-activated rice husk, ZnCl<sub>2</sub>-activated wood, acid-activated saw dust, ZnCl<sub>2</sub>-microwave-activated sawdust) [32,47,48]. The negative effect of initial Cr<sup>VI</sup> concentration is similar to the one observed in the process of Fe<sup>II</sup> removal, and has an identical explanation: the more rapid saturation of the reactive centers existent at surface of WSP-Fe<sup>0</sup> (available for the interaction with Cr<sup>VI</sup>) with increasing Cr<sup>VI</sup> concentration.

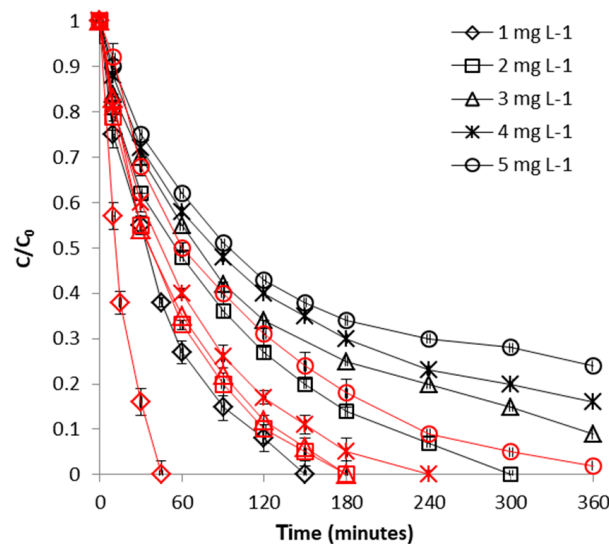


**Figure 10.** Effect of initial concentration on Cr<sup>VI</sup> removal by WSP-Fe<sup>0</sup> (red curves) and WSP (black curves). The lines are not fitting models; they simply connect points to facilitate visualization.

### 2.3.3. Effect of Temperature

The dependence of the Cr<sup>VI</sup> removal process with temperature was investigated over the range of 6–32 °C. It is evident from Figure 11 that removal of Cr<sup>VI</sup> with WSP-Fe<sup>0</sup> was highly dependent on the temperature: an increased trend in removal efficiency was noticed with rise in temperature, indicating the endothermic nature of the process. The observed influence of increasing temperature can be most probably ascribed to increase in rate of diffusion of the Cr<sup>VI</sup> ions across the boundary layer. Even though the same effect of temperature was observed also in control experiments with WSP (Figure 11), however, for same temperature, higher Cr<sup>VI</sup> removal efficiencies were always obtained for WSP-Fe<sup>0</sup> than for WSP, attributable to existence of Fe<sup>0</sup> at surface of WSP-Fe<sup>0</sup>. Our results are in line with previous findings indicating favorable binding of Cr<sup>VI</sup> on different biosorbents (acid-activated rice husk, ZnCl<sub>2</sub>-activated wood, acid-activated saw dust, ZnCl<sub>2</sub>-microwave-activated sawdust) at higher temperature [32,47,48].

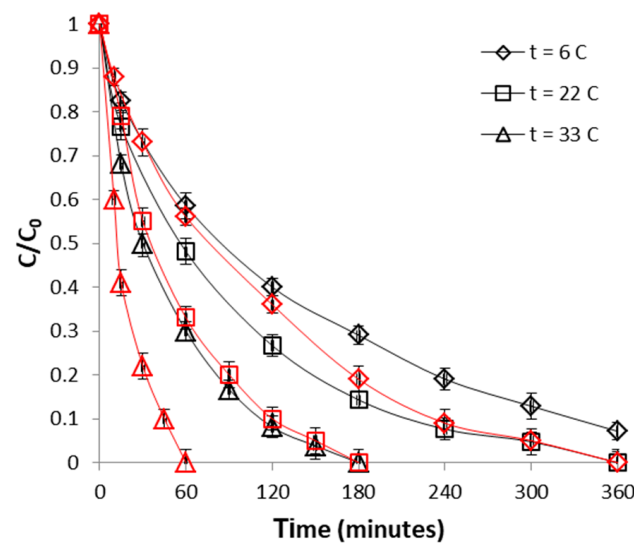


**Figure 11.** Effect of temperature on Cr<sup>VI</sup> removal by WSP-Fe<sup>0</sup> (red curves) and WSP (black curves). The lines are not fitting models; they simply connect points to facilitate visualization.

#### 2.3.4. Effect of Ionic Strength

To study the influence of this parameter, the ionic strength of Cr<sup>VI</sup> solutions was adjusted using NaCl as background electrolyte, in the concentration range of 0–0.05 M. The extent of Cr<sup>VI</sup> removal with WSP-Fe<sup>0</sup> as a function ionic strength is depicted in Figure 12. As revealed by this figure, the addition of NaCl (i.e., increase of ionic strength) led to a slight increase in Cr<sup>VI</sup> removal efficiency. The highest improvement in removal efficacy was noticed as the ionic strength was increased from 0 to 0.01 M; a further increase in ionic strength to 0.03 and 0.05 M lead to removal yields higher than for 0 M, but lower than for 0.01 M. Thus, it can be concluded that optimal ionic strength for Cr<sup>VI</sup> removal with WSP-Fe<sup>0</sup> was 0.01 M. On the other hand, control experiments conducted with WSP revealed that removal of Cr<sup>VI</sup> was practically not influenced by the increase of ionic strength (Figure 12). Conversely, other authors reported a more or less significant adverse influence of ionic strength on the removal of Cr<sup>VI</sup> with grape stalks, cork, olive stones, thermochemically-activated walnut shells or surfactant modified spent mushroom [46,53–55]. The two different effects exerted by the background ionic strength on removal of Cr<sup>VI</sup> with WSP-Fe<sup>0</sup> and with WSP are indicative of two distinct removal mechanisms involved in the two cases. On the one hand, the absence of any visible influence of ionic strength on Cr<sup>VI</sup> removal with WSP can be interpreted as indicating a specific adsorption mechanism [44]; on the other hand, the higher removal efficiencies obtained with WSP-Fe<sup>0</sup> at higher ionic strengths may be ascribed to existence of Fe<sup>0</sup> active sites at surface of WSP-Fe<sup>0</sup>. This is in accord with findings of previous studies which demonstrated that Cl<sup>-</sup> anion can accelerate Fe<sup>0</sup> corrosion by forming soluble complexes with Fe<sup>II</sup>, which are carried away from the metal surface; the as formed Fe<sup>II</sup> complexes have two important roles: (1) to delay the formation of oxide layers at surface of Fe<sup>0</sup>, and (2), to act as secondary reducing agents for the reduction of Cr<sup>VI</sup> [56,57].

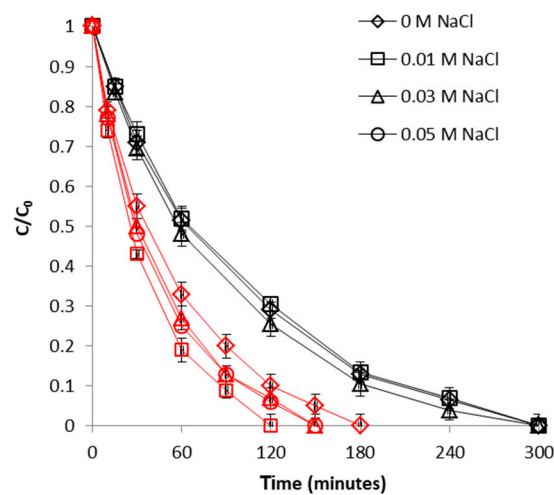


**Figure 12.** Effect of ionic strength on  $\text{Cr}^{\text{VI}}$  removal by WSP- $\text{Fe}^0$  (red curves) and WSP (black curves). The lines are not fitting models; they simply connect points to facilitate visualization.

## 2.4. Kinetic Modeling

### 2.4.1. Identification of the Kinetic Order

The statistical fits of  $\text{Fe}^{\text{II}}$  and  $\text{Cr}^{\text{VI}}$  removal experimental data to pseudo first and pseudo second-order equations, and the parameters of the two kinetic models are summarized in Table 1. With regard to  $\text{Fe}^{\text{II}}$  removal, as evidenced by the correlation coefficients, pseudo second-order kinetic model provided the best match for the experimental data. This conclusion is confirmed also by the fact that equilibrium adsorption capacity value ( $q_e$ ) predicted by the pseudo second-order model fits the best the experimental value ( $q_e^{\text{exp}}$ ). These evidences indicate that pseudo second-order kinetic model was the more appropriate to describe  $\text{Fe}^{\text{II}}$  adsorption. This is consistent with results from a previous study using thermochemically-activated orange peels [30]. The pseudo second-order kinetic model assumes that the rate-limiting step of the adsorption process is of chemisorption nature, involving sharing or exchange of electrons between adsorbent and adsorbate [58].

**Table 1.** Kinetic parameters of  $\text{Fe}^{\text{II}}$  and  $\text{Cr}^{\text{VI}}$  removal.

Test	Pseudo 1 <sup>st</sup> Order			Pseudo 2 <sup>nd</sup> Order			$q_e^{\text{exp}}$ ( $\text{mg g}^{-1}$ )
	$k_1$ ( $\text{min}^{-1}$ )	$q_e$ ( $\text{mg g}^{-1}$ )	$R^2$	$k_2$ ( $\text{g mg}^{-1} \text{min}^{-1}$ )	$q_e$ ( $\text{mg g}^{-1}$ )	$R^2$	
$\text{Fe}^{\text{II}}$ + WSP	$1.4 \times 10^{-3}$	1.20	0.7936	$18.8 \times 10^{-3}$	3.93	0.9998	4.20
$\text{Cr}^{\text{VI}}$ + WSP	$6.9 \times 10^{-3}$	0.35	0.9891	$1.9 \times 10^{-2}$	0.33	0.9874	0.40
$\text{Cr}^{\text{VI}}$ + WSP- $\text{Fe}^0$	$1.8 \times 10^{-2}$	0.46	0.9948	$5.9 \times 10^{-2}$	0.56	0.9923	0.50

From the kinetic data of  $\text{Cr}^{\text{VI}}$  removal with WSP- $\text{Fe}^0$  it can be seen that regression coefficient of the second-order model is lower than of the pseudo first-order model, which implies that removal of  $\text{Cr}^{\text{VI}}$  with WSP- $\text{Fe}^0$  follows the pseudo first-order kinetics. In addition, the calculated  $q_e$  value obtained from the pseudo first-order model agrees better with the experimental  $q_e^{\text{exp}}$  value than the one obtained from the second-order model. Consequently, the retention of  $\text{Cr}^{\text{VI}}$  onto WSP- $\text{Fe}^0$  could be best described by the pseudo first-order kinetic model. Control experiments with WSP are in good agreement with WSP- $\text{Fe}^0$  experiments, revealing that adsorption onto WSP also fitted well to the pseudo first-order kinetic model. The pseudo first-order kinetic model was successfully applied in early works investigating  $\text{Cr}^{\text{VI}}$  removal by different biomaterials (thermochemically-modified *Terminalia arjuna* nuts,  $\text{Fe}^{\text{III}}$  impregnated biochar and tea-waste [59–61]), being indicative for existence of relatively weak electrostatic interactions between  $\text{Cr}^{\text{VI}}$  and adsorbent [62]. Nevertheless,

several other studies, working with  $\text{ZnCl}_2$ -activated *S. guttata* shell waste or acid-activated pomegranate husk, indicated that pseudo-second order was the applicable kinetic model for  $\text{Cr}^{\text{VI}}$  removal [63,64].

#### 2.4.2. Identification of the Rate Limiting Step

Removal of a contaminant via adsorption occurs through a mechanism comprising the following consecutive steps: (1) transport of contaminant in the bulk of the solution, (2) transport of contaminant through the liquid film surrounding the adsorbent particle, to its external surface (film diffusion), (3) transport of contaminant from the adsorbent surface into its pores (intraparticle diffusion), and (4) retention of the contaminant inside the pores. Generally, phase (1) and (4) are very rapid and do not represent the rate determining step [65]. The Weber and Morris model was applied in this study to determine whether film diffusion or intraparticle diffusion is the rate limiting step. If intra-particle diffusion would be the rate-limiting step, then Weber and Morris plots should pass through the origin and have a good linearity. Figures 13–15 clearly reveal that, for both  $\text{Fe}^{\text{II}}$  and  $\text{Cr}^{\text{VI}}$  removal, the  $q_t$  versus  $t^{0.5}$  plots show multilinearity, indicating that at least two steps take place. This implies that intraparticle diffusion was not the only rate-controlling step, and that diffusion through the liquid film around the adsorbent toward particle surface is also involved in metal binding onto adsorbent. The first (sharper) region of the Weber and Morris plots corresponds to the phase of the adsorption which is predominantly controlled by film diffusion, while the second region describes the adsorption stage where intraparticle diffusion played the major role, being thus rate limiting [66,67]. Accordingly, the  $k_{\text{dif}}$  intraparticle diffusion rate constants were derived from the slope of the second linear portion, while the C values were computed from the intercept of the first linear portion. The  $k_{\text{dif}}$  intraparticle diffusion rate constant can be used for evaluation of the effect of intraparticle diffusion on the adsorption process: the higher the  $k_{\text{dif}}$ , the lower the resistance to diffusion inside the pores. The intercept C value provides information about the thickness of the boundary layer: the larger the intercept value, the greater the resistance of external mass transfer across the boundary layer [64,67].

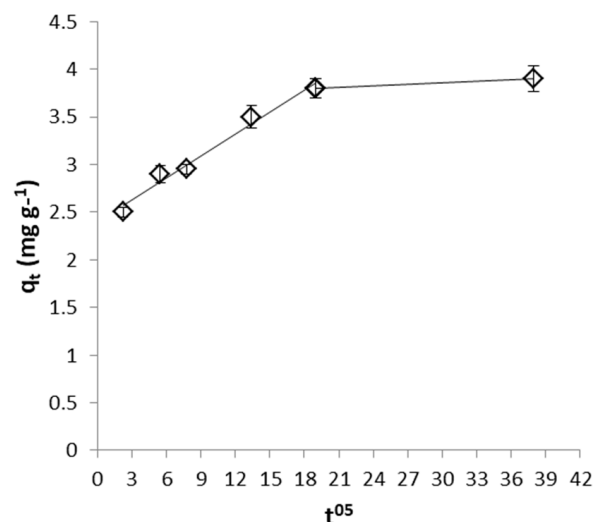


Figure 13. Weber and Morris plot for  $\text{Fe}^{\text{II}}$  removal by WSP.

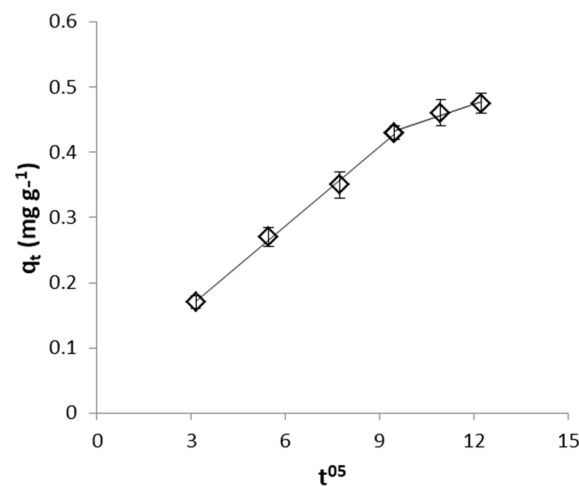


Figure 14. Weber and Morris plot for Cr<sup>VI</sup> removal by WSP-Fe<sup>0</sup>.

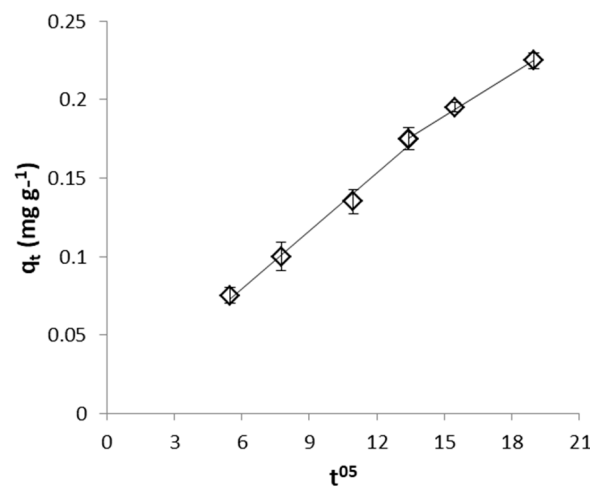


Figure 15. Weber and Morris plot for Cr<sup>VI</sup> removal by WSP.

From the values of intraparticle diffusion model parameters (Table 2) it can be seen that higher diffusion rate was observed for removal of Cr<sup>VI</sup> with WSP-Fe<sup>0</sup> than with WSP, while similar low C values were determined in both cases. On the other hand, Fe<sup>II</sup> removal with WSP is characterized by much lower diffusion rate constant and much higher boundary layer effect than removal of Cr<sup>VI</sup> with both WSP-Fe<sup>0</sup> and WSP. Similar Weber and Morris plots exhibiting multilinearity and not intersecting the origin were previously reported for the adsorption of acid-activated date palm seed, *Eichhornia crassipes* biomass and tea-waste [61,68,69].

Table 2. Weber and Morris diffusion model parameters.

	$k_{diff}$ (mg g <sup>-1</sup> min <sup>-0.5</sup> )	C
Fe <sup>II</sup> removal by WSP	$5.3 \times 10^{-3}$	2.4
Cr <sup>VI</sup> removal by WSP	$0.9 \times 10^{-2}$	$2 \times 10^{-2}$
Cr <sup>VI</sup> removal by WSP-Fe <sup>0</sup>	$1.6 \times 10^{-2}$	$3 \times 10^{-2}$

### 2.5. Mechanism of Metal Removal

The remediation of the AMD solution occurs through a pure adsorption process of Fe<sup>II</sup> at surface of WSP, via mixed physical and chemical mechanisms. Similarly, Cr<sup>VI</sup> removal with WSP-Fe<sup>0</sup> can also be ascribed to adsorption processes. However, in this case, the higher

removal efficiencies observed for WSP-Fe<sup>0</sup> than for WSP are indicative of existence of differences in mechanism of metal removal. This is attributable to Fe<sup>0</sup> centers formed at surface of WSP as a result of reaction between WSP-Fe<sup>II</sup> and sodium borohydride. Over the last three decades, Fe<sup>0</sup> has been demonstrated to represent a highly efficient reagent in remediation of water contaminated with a wide variety of pollutants, including Cr<sup>VI</sup>. Removal of Cr<sup>VI</sup> with Fe<sup>0</sup> occurs through a very complex mechanism, which may involve physicochemical processes such as adsorption, direct reduction, indirect reduction, co-precipitation/enmeshment in the mass of precipitates; generally, both adsorption and reduction processes of Cr<sup>VI</sup> in Fe<sup>0</sup>/H<sub>2</sub>O system are favored by an acidic pH, being strongly hindered at pH levels close to neutral values [45]. After being adsorbed at surface of WSP-Fe<sup>0</sup>, Cr<sup>VI</sup> can be reduced to Cr<sup>III</sup> by WSP functional groups, by Fe<sup>0</sup> (at very acidic pH, when it's not covered by oxides), by Fe<sup>II</sup>-based corrosion products formed at surface of Fe<sup>0</sup> or by dissolved Fe<sup>II</sup>. In addition, under acidic conditions, Cr<sup>VI</sup> reduction may take place also homogeneously with dissolved Fe<sup>II</sup>. Thus, we can suggest that removal of Cr<sup>VI</sup> with WSP-Fe<sup>0</sup> occurred through a combined adsorption-reduction process. However, since very low concentrations of dissolved Cr<sup>III</sup> (~0.2–0.4 mg L<sup>-1</sup>) were detected only at pH 1.0 and 2.1, and Cr<sup>III</sup> adsorption/precipitation is inhibited at acidic pH, it can be assumed that adsorption processes played the most important role in removal of Cr<sup>VI</sup>. This is in good agreement with similar observations reported by other researchers, indicating that Cr<sup>VI</sup> removal by natural biomaterials occurs via an adsorption-coupled reduction mechanism [70,71].

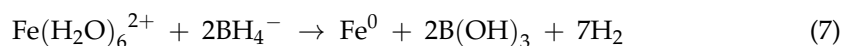
### 3. Materials and Methods

#### 3.1. Preparation of the Adsorbent for AMD Treatability Experiments

Walnuts (*Juglans regia*) were obtained from a local market in Timisoara (Romania). After crushing the walnuts by hand, shells were separated, rinsed several times with distilled water to remove impurities, and dried in an oven at 80 °C for 24 h. Then, the dried shells were powdered using an electric grinder. The resultant WSP was washed with distilled water until no brown coloration of the water was noticed, and then dried again in oven at 80 °C for 24 h, to remove moisture. After cooling, the WSP was ground with a mortar and pestle, and subsequently sieved to particles size of 0.5–1.25 mm for further treatability experiments with synthetic AMD solutions.

#### 3.2. Preparation of the Reactive Material for Cr<sup>VI</sup> Treatability Experiments

After each AMD treatability experiment, the exhausted adsorbent (WSP-Fe<sup>II</sup>) was recovered and dried at room temperature. By means of mass balance calculation, the concentration of adsorbed iron was determined to be about 3 mg Fe<sup>II</sup>/g WSP. Then, the adsorbed Fe<sup>II</sup> was reduced to Fe<sup>0</sup> via the liquid-phase reduction method, using sodium borohydride (NaBH<sub>4</sub>) as reducing reagent [72]:



About 250 mL distilled water were added over 80 g of WSP-Fe<sup>II</sup> and the obtained slurry was stirred at a rate of 200 rpm, in order to keep solid particles in suspension. Then, 0.6 g NaBH<sub>4</sub> was added in small portions while stirring, in a fume hood; NaBH<sub>4</sub> was used in excess to the stoichiometric needed amount, in order to account for any that may decompose during the course of the reaction with water. The usual brown color of the solid material immediately darkened to a black appearance, indicating the formation of Fe<sup>0</sup> centers at surface of WSP (Figure S16) [73]. After the addition of NaBH<sub>4</sub> was completed (~60 min), the resulted mixture was stirred for an additional 60 min. The resulted WSP-Fe<sup>0</sup> was separated from the solution, washed with distilled water, dried at 80 °C for 24 h in an oven, and kept in vacuum desiccator prior to being used in treatability experiments with Cr<sup>VI</sup> solution.

### 3.3. AMD Treatability Experiments

Synthetic AMD stock solution (1000 mg L<sup>-1</sup>) was prepared by dissolving the required amount of AR grade FeSO<sub>4</sub>·7H<sub>2</sub>O in distilled de-ionized water. Then, AMD working solutions with desired Fe<sup>II</sup> concentrations were prepared by appropriate dilution of stock solution, knowing that Fe is often the main heavy metal present in acid mine drainage [74]. AMD treatability experiments were conducted in batch system, using an Ovan jar tester. 500 mL AMD solution was poured in 800 mL Berzelius flasks, followed by addition of 5 g WSP. The mixture was stirred (200 rpm) and, at timed intervals, samples were withdrawn, filtered using a 0.45 µm filter and analyzed for Fe<sup>II</sup>. The pH of Fe<sup>II</sup> solutions was adjusted before experiments to the required value by addition of small amounts of concentrated H<sub>2</sub>SO<sub>4</sub>. Detailed conditions of AMD treatability experiments are summarized in Table 3.

**Table 3.** Setup design of AMD treatability experiments

	Investigation of the Influence of			
	pH	Fe <sup>II</sup> Concentration	Temperature	Ionic Strength
pH	1.0–4.1	4.1	4.1	4.1
Fe <sup>II</sup> concentration (mg L <sup>-1</sup> )	50	25–100	50	50
Temperature (°C)	22	22	6–33	22
Ionic strength (mole L <sup>-1</sup> NaCl)	0	0	0	0–0.05

### 3.4. Cr<sup>VI</sup> Treatability Experiments

Cr<sup>VI</sup> stock solution (1000 mg L<sup>-1</sup>) was prepared by dissolving the required amount of AR grade K<sub>2</sub>Cr<sub>2</sub>O<sub>7</sub> in distilled de-ionized water. The stock solution was then further diluted with de-ionized distilled water in order to prepare the working Cr<sup>VI</sup> solutions. Batch Cr<sup>VI</sup> treatability experiments were conducted by mixing 1 g of WSP-Fe<sup>0</sup> with a volume 500 of mL Cr<sup>VI</sup> solution in 800 mL Berzelius flasks. The mixture was stirred using an Ovan jar tester (200 rpm) and, at predetermined times, supernatant aliquots were collected, filtered through a 0.45 µm filter and sent to Cr<sup>VI</sup> analysis. The pH of Cr<sup>VI</sup> solution was set by addition of small amounts of concentrated H<sub>2</sub>SO<sub>4</sub> or 1 M NaOH solution. For comparison purposes, control Cr<sup>VI</sup> treatability experiments with raw WSP were also conducted, by keeping unchanged all experimental conditions. Detailed conditions of Cr<sup>VI</sup> treatability experiments are summarized in Table 4.

**Table 4.** Setup design of Cr<sup>VI</sup> treatability experiments

	Investigation of the Influence of			
	pH	Cr <sup>VI</sup> Concentration	Temperature	Ionic Strength
pH	1.0–5.9	3.0	3.0	3.0
Cr <sup>VI</sup> concentration (mg L <sup>-1</sup> )	2	1–5	2	2
Temperature (°C)	22	22	6–33	22
Ionic strength (mole L <sup>-1</sup> NaCl)	0	0	0	0–0.05

### 3.5. Analytical Procedure

Cr<sup>VI</sup> and Fe<sup>II</sup> concentrations in the filtrate were analyzed by the 1,5-diphenylcarbazide method (at 540 nm) and, 1,10-orthophenantroline colorimetric method (at 510 nm), respectively, by using a 200 PLUS spectrophotometer (Specord, Germany). Cr<sup>total</sup> was determined

by treating the sample with  $\text{KMnO}_4$  to oxidize any present  $\text{Cr}^{\text{III}}$ , followed by analysis as  $\text{Cr}^{\text{VI}}$ ; then,  $\text{Cr}^{\text{III}}$  was determined from the difference between  $\text{Cr}^{\text{total}}$  and  $\text{Cr}^{\text{VI}}$  [75]. The pH of the samples was measured using a 7320 pH-meter (Inolab, Germany); three standard buffer solutions at pHs 4.0, 7.0 and 10.0 were employed for calibration. Point of zero charge ( $\text{pH}_{\text{pzc}}$ ) of WSP surface was determined using the pH drift method [76]. The prepared adsorbents were characterized by Fourier transform infrared spectrometry (FTIR: VERTEX 70, Bruker, Germany) and scanning electron microscopy (SEM: Inspect S, FEI, The Netherlands) coupled with energy dispersive X-ray spectroscopy (EDX: GENESIS XM 2i, The Netherlands).

### 3.6. Kinetic Modeling of Experimental Data

The kinetics of contaminant removal was analyzed using the linearized forms of Lagergren pseudo first-order model and Ho's pseudo second-order model [58,77,78]:

$$\log(q_e - q_t) = \log q_e - \frac{k_1}{2303} t \quad (8)$$

$$\frac{t}{q_t} = \frac{1}{k_2 q_e^2} + \frac{t}{q_e} \quad (9)$$

where  $q_e$  is the equilibrium adsorption capacity ( $\text{mg g}^{-1}$ ),  $q_t$  is the adsorption capacity at time  $t$  ( $\text{mg g}^{-1}$ ),  $k_1$  ( $\text{min}^{-1}$ ) and  $k_2$  ( $\text{g mg}^{-1} \text{min}^{-1}$ ) are the pseudo first-order and, respectively, pseudo second-order adsorption rate coefficients. The product  $k_2 q_e^2$  also represents the initial sorption rate.  $q_e$  and  $q_t$  were calculated as follows:

$$q_t = \frac{(C_0 - C_t)V}{M} \quad (10)$$

$$q_e = \frac{(C_0 - C_e)V}{M} \quad (11)$$

where  $M$  is the mass of adsorbent used in the kinetic experiments (g),  $C_e$  the equilibrium concentration of metal ( $\text{mg L}^{-1}$ ),  $C_t$  the metal concentration at time  $t$  ( $\text{mg L}^{-1}$ ),  $C_0$  the initial concentration of metal ( $\text{mg L}^{-1}$ );  $V$  the volume of solution used in the kinetic experiments (L).

The slope and intercept of the plots of  $\log(q_e - q_t)$  vs.  $t$  allows computation of pseudo first-order  $k_1$  and of equilibrium adsorption capacity  $q_e$ ; similarly, the plot of  $t/q_t$  vs.  $t$  enables the pseudo second-order rate constant  $k_2$  and  $q_e$  to be determined from intercept and slope. In order to further assess the nature of the rate-limiting step of the process (film diffusion or intraparticle diffusion), experimental data was fitted also to the Weber and Morris intraparticle diffusion model [64,79]:

$$q_t = k_{\text{diff}} \cdot t^{0.5} + C \quad (12)$$

where  $q_t$  ( $\text{mg g}^{-1}$ ) is the adsorption capacity at time  $t$ ,  $k_{\text{diff}}$  ( $\text{mg g}^{-1} \text{min}^{-0.5}$ ) is the intraparticle diffusion rate constant and  $C$  is a constant linked to the apparent thickness of the film boundary layer.

Kinetic modeling was conducted using experimental data acquired at pH 4.1,  $50 \text{ mg L}^{-1}$ ,  $22 \text{ }^\circ\text{C}$ , and pH 4.1,  $2 \text{ mg L}^{-1}$ ,  $22 \text{ }^\circ\text{C}$ , for  $\text{Fe}^{\text{II}}$  and  $\text{Cr}^{\text{VI}}$ , respectively.

### 3.7. Statistical Analysis

All the data represent the mean of two independent experiments and relative error less than 2% were obtained. Statistical analysis was performed using Microsoft Excel 2016 statistical tool.

## 4. Conclusions

In last years, the use of agricultural wastes/byproducts as cost-effective alternative adsorbents for the treatment of water contaminated with a large variety of pollutants

has attracted significant interest. However, much less interest has shown for finding environmentally-friendly solutions for the management of residual solids resulted from such water treatment processes. The present paper presents data on the use of WSP, a local agricultural waste, for the sequential removal of two heavy metals, namely Fe<sup>II</sup> and Cr<sup>VI</sup>, from aqueous effluents. Results presented herein clearly demonstrated that WSP can be considered as a promising adsorbent for the removal of Fe<sup>II</sup> from AMD, while WSP-Fe<sup>0</sup>, obtained by treating the Fe<sup>II</sup>-contaminated solid residue (WSP-Fe<sup>II</sup>) with sodium borohydride, is a suitable reactive reagent in the process of Cr<sup>VI</sup> removal from contaminated waters. The better capacity of WSP-Fe<sup>0</sup> to remove Cr<sup>VI</sup>, compared to fresh WSP, was ascribed to existence of Fe<sup>0</sup> centers at surface of WSP-Fe<sup>0</sup>. Adsorption kinetics of Cr<sup>VI</sup> and Fe<sup>II</sup> was successfully fitted by the pseudo first- and pseudo second-order model, respectively. While binding of Fe<sup>II</sup> on WSP occurred via physical and chemical mixed adsorption, removal of Cr<sup>VI</sup> with WSP-Fe<sup>0</sup> took place through a more complex mechanism, involving both adsorption and reduction processes. This study provides compelling evidence that residues resulted from a water adsorption treatment process can be successfully converted into reactive materials for a subsequent water treatment technology. The major challenge of this strategy is to identify water treatment processes with fully compatible pollutants.

**Supplementary Materials:** The following are available online at <https://www.mdpi.com/2227-9717/9/2/218/s1>.

**Author Contributions:** Conceptualization, M.G. and I.B.; methodology, M.G. and I.B.; software, M.G.; validation, M.G. and I.B.; formal analysis, M.G. and I.B.; investigation, M.G. and I.B.; resources, M.G. and I.B.; data curation, M.G. and I.B.; writing—original draft preparation, M.G.; writing—review and editing, M.G. and I.B.; visualization, M.G. and I.B.; supervision, M.G. All authors have read and agreed to the published version of the manuscript.

**Funding:** This research received no external funding.

**Institutional Review Board Statement:** Not applicable.

**Informed Consent Statement:** Not applicable.

**Data Availability Statement:** Data is contained within the article.

**Acknowledgments:** We sincerely thank the three anonymous reviewers from Processes whose insightful comments and suggestions provided on earlier version of this manuscript helped improve and clarify this study.

**Conflicts of Interest:** The authors declare no conflict of interest.

## References

1. Vardhan, K.H.; Kumar, P.S.; Panda, R.C. A review on heavy metal pollution, toxicity and remedial measures: Current trends and future perspectives. *J. Mol. Liq.* **2019**, *290*, 111197. [CrossRef]
2. Bozic, D.; Stankovic, V.; Gorgievski, M.; Bogdanovic, G.; Kovacevic, R. Adsorption of heavy metal ions by sawdust of deciduous trees. *J. Hazard. Mater.* **2009**, *171*, 684–692. [CrossRef] [PubMed]
3. Barakat, M.A. New trends in removing heavy metals from industrial wastewater. *Arab. J. Chem.* **2011**, *4*, 361–377. [CrossRef]
4. Gautam, R.K.; Mudhoo, A.; Lofrano, G.; Chattopadhyaya, M.C. Biomass-derived biosorbents for metal ions sequestration: Adsorbent modification and activation methods and adsorbent regeneration. *J. Environ. Chem. Eng.* **2014**, *2*, 239–259. [CrossRef]
5. Akhbarizadeh, R.; Shayestefar, M.R.; Darezereshki, E. Competitive removal of metals from wastewater by maghemite nanoparticles: A comparison between simulated wastewater and AMD. *Mine Water Environ.* **2014**, *33*, 89–96. [CrossRef]
6. Gheju, M.; Pode, R.; Manea, F. Comparative heavy metal chemical extraction from anaerobically digested biosolids. *Hydrometallurgy* **2011**, *108*, 115–121. [CrossRef]
7. Fu, F.; Wang, Q. Removal of heavy metal ions from wastewaters: A review. *J. Environ. Manag.* **2011**, *92*, 407–418. [CrossRef]
8. Bolisetty, S.; Peydayesh, M.; Mezzenga, R. Sustainable technologies for water purification from heavy metals: Review and analysis. *Chem. Soc. Rev.* **2019**, *48*, 463–487. [CrossRef]
9. Hashim, M.A.; Mukhopadhyay, S.; Sahu, J.N.; Sengupta, B. Remediation technologies for heavy metal contaminated groundwater. *J. Environ. Manag.* **2011**, *92*, 2355–2388. [CrossRef]

10. Selvi, A.; Rajasekar, A.; Theerthagiri, J.; Ananthaselvam, A.; Sathishkumar, K.; Madhavan, J.; Rahman, P.K.S.M. Integrated remediation processes toward heavy metal removal/recovery from various environments—A review. *Front. Environ. Sci.* **2019**, *7*, 66. [[CrossRef](#)]
11. Hu, M.; Zhang, S.; Pan, B.; Zhang, W.; Lv, L.; Zhang, Q. Heavy metal removal from water/wastewater by nanosized metal oxides: A review. *J. Hazard. Mater.* **2012**, *211–212*, 317–331. [[CrossRef](#)] [[PubMed](#)]
12. Kurniawan, T.A.; Chan, G.Y.S.; Lo, W.H.; Babel, S. Comparisons of low-cost adsorbents for treating wastewaters laden with heavy metals. *Sci. Total Environ.* **2006**, *366*, 409–426. [[CrossRef](#)] [[PubMed](#)]
13. Heidarinejad, Z.; Dehghani, M.H.; Heidari, M.; Javedan, G.; Ali, I.; Sillanpää, M. Methods for preparation and activation of activated carbon: A review. *Environ. Chem. Lett.* **2019**, *18*, 393–415. [[CrossRef](#)]
14. Dias, J.M.; Alvim-Ferraz, M.C.M.; Almeida, M.F.; Rivera-Utrilla, J.; Sanchez-Polo, M. Waste materials for activated carbon preparation and its use in aqueous-phase treatment: A review. *J. Environ. Manag.* **2007**, *85*, 833–846. [[CrossRef](#)]
15. Sirry, S.M.; Aldakhil, F.; Alharbi, O.M.L.; Ali, I. Chemically treated date stones for uranium (VI) uptake and extraction in aqueous solutions. *J. Mol. Liq.* **2019**, *273*, 192–202. [[CrossRef](#)]
16. Mosoarca, G.; Vancea, C.; Popa, S.; Gheju, M.; Boran, S. Syringa vulgaris leaves powder a novel low-cost adsorbent for methylene blue removal: Isotherms, kinetics, thermodynamic and optimization by Taguchi method. *Sci. Rep.* **2020**, *10*, 17676. [[CrossRef](#)]
17. Abdel-Ghani, N.T.; El-Chaghaby, G.A. Biosorption for metal ions removal from aqueous solutions: A review of recent studies. *Int. J. Lat. Res. Sci. Technol.* **2014**, *3*, 24–42.
18. Mohan, D.; Pittman, C.U., Jr. Activated carbons and low cost adsorbents for remediation of tri- and hexavalent chromium from water. *J. Hazard. Mater.* **2006**, *B137*, 762–811. [[CrossRef](#)]
19. Joseph, L.; Jun, B.M.; Flora, J.R.V.; Park, C.M.; Yoon, Y. Removal of heavy metals from water sources in the developing world using low-cost materials: A review. *Chemosphere* **2019**, *229*, 142–159. [[CrossRef](#)]
20. Ahmad, T.; Ahmad, K.; Alam, M. Sustainable management of water treatment sludge through 3'R' concept. *J. Clean. Prod.* **2016**, *124*, 1–13. [[CrossRef](#)]
21. Ippolito, J.A.; Barbarick, K.A.; Elliott, H.A. Drinking water treatment residuals: A review of recent uses. *J. Environ. Qual.* **2011**, *40*, 1–12. [[CrossRef](#)]
22. Turner, T.; Wheeler, R.; Stone, A.; Oliver, I. Potential alternative reuse pathways for water treatment residuals: Remaining barriers and questions—A Review. *Water Air Soil Pollut.* **2019**, *230*, 227. [[CrossRef](#)]
23. Babatunde, A.; Zhao, Y. Constructive approaches toward water treatment works sludge management: An international review of beneficial reuses. *Crit. Rev. Environ. Sci. Technol.* **2007**, *37*, 129–164. [[CrossRef](#)]
24. Wolowicz, M.; Komorowska-Kaufman, M.; Pruss, A.; Rzepam, G.; Bajda, T. Removal of heavy metals and metalloids from water using drinking water treatment residuals as adsorbents: A review. *Minerals* **2019**, *9*, 487. [[CrossRef](#)]
25. Gheju, M.; Balcu, I. Mitigation of Cr(VI) aqueous pollution by reuse of iron-contaminated water treatment residues. *ChemEngineering* **2017**, *1*, 9. [[CrossRef](#)]
26. Sagar, N.A.; Pareek, S.; Sharma, S.; Yahia, E.M.; Lobo, M.G. Fruit and vegetable waste: Bioactive compounds, their extraction, and possible utilization. *Compr. Rev. Food Sci. Food Saf.* **2018**, *17*, 512–531. [[CrossRef](#)]
27. Gowe, C. Review on potential use of fruit and vegetables by-products as a valuable source of natural food additives. *Food Sci. Qual. Manag.* **2015**, *45*, 47–61.
28. USDA. *Tree nuts: World Market and Trade*; United States Department of Agriculture Foreign Agricultural Service: Washington, DC, USA, 2017.
29. Ghasemi, M.; Ghoreyshi, A.A.; Younesi, H.; Khoshhal, S. Synthesis of a high characteristics activated carbon from walnut shell for the removal of Cr(VI) and Fe(II) from aqueous solution: Single and binary solutes adsorption. *Iran. J. Chem. Eng.* **2015**, *12*, 28–51.
30. Adebayo, G.B.; Mohammed, A.A.; Sokoya, S.O. Biosorption of Fe(II) and Cd(II) ions from aqueous solution using a low cost adsorbent from orange peels. *J. Appl. Sci. Environ. Manag.* **2016**, *20*, 702–714. [[CrossRef](#)]
31. Noubactep, C. Metallic iron for environmental remediation: A review of reviews. *Water Res.* **2015**, *85*, 114–123. [[CrossRef](#)]
32. Bansal, M.; Singh, D.; Garg, V.K. A comparative study for the removal of hexavalent chromium from aqueous solution by agriculture wastes' carbons. *J. Hazard. Mater.* **2009**, *171*, 83–92. [[CrossRef](#)] [[PubMed](#)]
33. Savy, D.; Piccolo, A. Physical-chemical characteristics of lignins separated from biomasses for second-generation ethanol. *Biomass Bioenergy* **2014**, *62*, 58–67. [[CrossRef](#)]
34. Coates, J. Interpretation of infrared spectra, a practical approach. In *Encyclopedia of Analytical Chemistry*; Meyers, R.A., Ed.; John Wiley & Sons: Chichester, UK, 2000; pp. 10815–10837.
35. Domínguez-Robles, J.; Sánchez, R.; Espinosa, E.; Savy, D.; Mazzei, P.; Piccolo, A.; Rodríguez, A. Isolation and characterization of *Gramineae* and *Fabaceae* soda lignins. *Int. J. Mol. Sci.* **2017**, *18*, 327. [[CrossRef](#)] [[PubMed](#)]
36. Aravindhan, R.; Madhan, B.; Rao, J.R.; Nair, B.U.; Ramasam, T. Bioaccumulation of chromium from tannery wastewater: An approach for chrome recovery and reuse. *Environ. Sci. Technol.* **2004**, *38*, 300–306. [[CrossRef](#)] [[PubMed](#)]
37. Bykov, I. Characterization of Natural and Technical Lignins Using FTIR Spectroscopy. Master's Thesis, Lulea University of Technology, Lulea, Sweden, 2008.
38. Bhattacharyya, K.G.; Sen Gupta, S. Adsorption of chromium(VI) from water by clays. *Ind. Eng. Chem. Res.* **2006**, *45*, 7232–7240. [[CrossRef](#)]

39. Espana, J.S.; Pamo, E.L.; Pastor, E.S. The oxidation of ferrous iron in acidic mine effluents from the Iberian Pyrite Belt (Odiel Basin, Huelva, Spain): Field and laboratory rates. *J. Geochem. Explor.* **2007**, *92*, 120–132. [[CrossRef](#)]
40. Espana, J.S. Acid mine drainage in the Iberian pyrite belt: An overview with special emphasis on generation mechanisms, aqueous composition and associated mineral phases. *Macla* **2008**, *10*, 34–43.
41. Yu, L.J.; Shukla, S.S.; Doris, K.L.; Shukla, A.; Margrave, J.L. Adsorption of chromium from aqueous solutions by maple sawdust. *J. Hazard. Mater* **2003**, *B100*, 53–63. [[CrossRef](#)]
42. Baral, S.S.; Das, S.N.; Rath, P. Hexavalent chromium removal from aqueous solution by adsorption on treated sawdust. *Biochem. Eng. J.* **2006**, *31*, 216–222. [[CrossRef](#)]
43. Das, D.D.; Mahapatra, R.; Pradhan, J.; Das, S.N.; Thakur, R.S. Removal of Cr(VI) from aqueous solution using activated cow dung carbon. *J. Coll. Interf. Sci.* **2000**, *232*, 235–240. [[CrossRef](#)]
44. McBride, M.B. A critique of diffuse double layer models applied to colloid and surface chemistry. *Clays Clay Miner.* **1997**, *45*, 598–608. [[CrossRef](#)]
45. Gheju, M. Decontamination of hexavalent chromium-polluted waters: Significance of metallic iron technology. In *Enhancing Cleanup of Environmental Pollutants. Volume 2. Non biological Approaches*; Anjum, N., Gill, S., Tuteja, N., Eds.; Springer International Publishing: Cham, Switzerland, 2017; pp. 209–254.
46. Albadarin, A.B.; Mangwandi, C.; Walker, G.M.; Allen, S.J.; Ahmad, M.N.M.; Khraisheh, M. Influence of solution chemistry on Cr(VI) reduction and complexation onto date-pits/tea-waste biomaterials. *J. Environ. Manag.* **2013**, *114*, 190–201. [[CrossRef](#)] [[PubMed](#)]
47. Acharya, J.; Sahu, J.N.; Sahoo, B.K.; Mohanty, C.R.; Meikap, B.C. Removal of chromium(VI) from wastewater by activated carbon developed from Tamarind wood activated with zinc chloride. *Chem. Eng. J.* **2009**, *150*, 25–39. [[CrossRef](#)]
48. Chen, C.; Zhao, P.; Li, Z.; Tong, Z. Adsorption behavior of chromium(VI) on activated carbon from eucalyptus sawdust prepared by microwave-assisted activation with ZnCl<sub>2</sub>. *Desal. Water Treat.* **2016**, *57*, 12572–12584. [[CrossRef](#)]
49. Amuda, O.S.; Adelowo, F.E.; Ologunde, M.O. Kinetics and equilibrium studies of adsorption of chromium(VI) ion from industrial wastewater using *Chrysothryllum albidum* (Sapotaceae) seed shells. *Colloids Surf. B Biointerfaces* **2009**, *68*, 184–192. [[CrossRef](#)]
50. Flury, B.; Eggenberger, U.; Mader, U. First results of operating and monitoring an innovative design of a permeable reactive barrier for the remediation of chromate contaminated groundwater. *J. Appl. Geochem.* **2009**, *24*, 687–697. [[CrossRef](#)]
51. Gao, R.M. Simultaneous determination of hexavalent and total chromium in water and plating baths by spectrophotometry. *Talanta* **1993**, *40*, 637–640. [[CrossRef](#)]
52. Ye, J.; Yin, H.; Mai, B.; Peng, H.; Qin, H.; He, B.; Zhang, N. Biosorption of chromium from aqueous solution and electroplating wastewater using mixture of *Candida lipolytica* and dewatered sewage sludge. *Biores. Technol.* **2010**, *101*, 3893–3902. [[CrossRef](#)]
53. Altun, T.; Pehlivan, E. Removal of Cr(VI) from aqueous solutions by modified walnut shells. *Food Chem.* **2012**, *132*, 693–700. [[CrossRef](#)]
54. Fiol, N.; Villaescusa, I.; Martinez, M.; Miralles, N.; Poch, J.; Serarols, J. Biosorption of Cr(VI) using low cost sorbents. *Environ. Chem. Lett.* **2003**, *1*, 135–139. [[CrossRef](#)]
55. Jing, X.; Cao, Y.; Zhang, X.; Wang, D.; Wu, X.; Xu, H. Biosorption of Cr(VI) from simulated wastewater using a cationic surfactant modified spent mushroom. *Desalination* **2011**, *269*, 120–127. [[CrossRef](#)]
56. Tepong-Tsindé, R.; Phukan, M.; Nassi, A.; Noubactep, C.; Ruppert, H. Validating the Efficiency of the MB Discoloration Method for the Characterization of Fe<sup>0</sup>/H<sub>2</sub>O systems using accelerated corrosion by chloride ions. *Chem. Eng. J.* **2015**, *279*, 353–362. [[CrossRef](#)]
57. Gheju, M.; Balcu, I.; Enache, A.; Flueraș, A. A kinetic approach on hexavalent chromium removal with metallic iron. *J. Environ. Manag.* **2017**, *203*, 937–941. [[CrossRef](#)] [[PubMed](#)]
58. Mohan, D.; Singh, K.P.; Singh, V.K. Removal of hexavalent chromium from aqueous solution using low-cost activated carbons derived from agricultural waste materials and activated carbon fabric cloth. *Ind. Eng. Chem. Res.* **2005**, *44*, 1027–1042. [[CrossRef](#)]
59. Wang, H.; Tian, Z.; Jiang, L.; Luo, W.; Wei, Z.; Li, S.; Cui, J.; Wei, W. Highly efficient adsorption of Cr(VI) from aqueous solution by Fe<sup>3+</sup> impregnated biochar. *J. Disp. Sci. Technol.* **2017**, *38*, 815–825. [[CrossRef](#)]
60. Mohanty, K.; Jha, M.; Meikap, B.C.; Biswas, M.N. Removal of chromium (VI) from dilute aqueous solutions by activated carbon developed from *Terminalia arjuna* nuts activated with zinc chloride. *Chem. Eng. Sci.* **2005**, *60*, 3049–3059. [[CrossRef](#)]
61. Malkoc, E.; Nuhoglu, Y. Potential of tea factory waste for chromium(VI) removal from aqueous solutions: Thermodynamic and kinetic studies. *Sep. Purif. Technol.* **2007**, *54*, 291–298. [[CrossRef](#)]
62. Maitlo, H.A.; Kim, K.H.; Kumar, V.; Kim, S.; Park, J.W. Nanomaterials-based treatment options for chromium in aqueous environments. *Environ. Int.* **2019**, *130*, 104748. [[CrossRef](#)]
63. Rangabhashiyam, S.; Selvaraju, N. Adsorptive remediation of hexavalent chromium from synthetic wastewater by a natural and ZnCl<sub>2</sub> activated *Sterculia guttata* shell. *J. Molec. Liq.* **2015**, *207*, 39–49. [[CrossRef](#)]
64. El Nemr, A. Potential of pomegranate husk carbon for Cr(VI) removal from wastewater: Kinetic and isotherm studies. *J. Hazard. Mater.* **2009**, *161*, 132–141. [[CrossRef](#)]
65. Zhu, Q.; Moggridge, G.D.; D'Agostino, C. Adsorption of pyridine from aqueous solutions by polymeric adsorbents MN 200 and MN 500. Part 2: Kinetics and diffusion analysis. *Chem. Eng. J.* **2016**, *306*, 1223–1233. [[CrossRef](#)]
66. Golban, A.; Lupa, L.; Cocheci, L.; Pode, R. Synthesis of MgFe layered double hydroxide from iron-containing acidic residual solution and its adsorption performance. *Crystals* **2019**, *9*, 514. [[CrossRef](#)]

67. Khambhaty, Y.; Mody, K.; Basha, S.; Jha, B. Kinetics, equilibrium and thermodynamic studies on biosorption of hexavalent chromium by dead fungal biomass of marine *Aspergillus niger*. *Chem. Eng. J.* **2009**, *145*, 489–495. [[CrossRef](#)]
68. El Nemr, A.; Khaled, A.; Abdelwahab, O.; El-Sikaily, A. Treatment of wastewater containing toxic chromium using new activated carbon developed from date palm seed. *J. Hazard. Mater.* **2009**, *152*, 263–275. [[CrossRef](#)] [[PubMed](#)]
69. Mohanty, K.; Jha, M.; Meikap, B.C.; Biswas, M.N. Biosorption of Cr(VI) from aqueous solutions by *Eichhornia crassipes*. *Chem. Eng. J.* **2006**, *117*, 71–77. [[CrossRef](#)]
70. Park, D.; Lim, S.R.; Yun, Y.S.; Park, J.M. Reliable evidences that the removal mechanism of hexavalent chromium by natural biomaterials is adsorption-coupled reduction. *Chemosphere* **2007**, *70*, 298–305. [[CrossRef](#)]
71. Lin, Y.C.; Wang, S.L. Cr K-edge X-ray absorption and FTIR spectroscopic study on the reaction mechanisms of Cr(III) and Cr(VI) with lignin. *Desal. Water Treat.* **2016**, *57*, 21598–21609. [[CrossRef](#)]
72. Uzum, C.; Shahwan, T.; Eroglu, A.E.; Lieberwirth, I.; Scott, T.B.; Hallam, K.R. Application of zero-valent iron nanoparticles for the removal of aqueous Co<sup>2+</sup> ions under various experimental conditions. *Chem. Eng. J.* **2008**, *144*, 213–220. [[CrossRef](#)]
73. Ali, S.W.; Mirza, M.L.; Bhatti, T.M. Removal of Cr(VI) using iron nanoparticles supported on porous cation-exchange resin. *Hydrometallurgy* **2015**, *157*, 82–89. [[CrossRef](#)]
74. Rakotonimaro, T.V.; Neculita, C.M.; Bussiere, B.; Zagury, G.J. Comparative column testing of three reactive mixtures for the bio-chemical treatment of iron-rich acid mine drainage. *Miner. Eng.* **2017**, *111*, 79–89. [[CrossRef](#)]
75. APHA, AWWA, WEF. *Standard Methods for the Examination of Water and Wastewater*, 19th ed.; United Book Press: Baltimore, MD, USA, 1995.
76. Zach-Maor, A.; Semiat, R.; Shemer, H. Synthesis, performance, and modeling of immobilized nano-sized magnetite layer for phosphate removal. *J. Colloid Interface Sci.* **2011**, *357*, 440–446. [[CrossRef](#)] [[PubMed](#)]
77. Cocheci, L.; Pode, R.; Popovici, E.; Dvininov, E.; Iovi, A. Sorption removal of chromate in single batch systems by uncalcined and calcined Mg/Zn-Al-type hydrotalcites. *Environ. Eng. Manag. J.* **2009**, *8*, 865–870. [[CrossRef](#)]
78. Ho, Y.S. Review of second-order models for adsorption systems. *J. Hazard. Mater.* **2006**, *B136*, 681–689. [[CrossRef](#)] [[PubMed](#)]
79. Albadarin, A.B.; Mangwandi, C.; Al-Muhtase, A.H.; Walker, G.M.; Allen, S.J.; Ahmad, M.N.M. Kinetic and thermodynamics of chromium ions adsorption onto low-cost dolomite adsorbent. *Chem. Eng. J.* **2012**, *179*, 193–202. [[CrossRef](#)]